*Journal of the Korean Nuclear Society*
*Volume 33, Number 4, pp.344~357, August, 2002*

# Spontaneous Steam Explosions Observed In The Fuel Coolant Interaction Experiments Using Reactor Materials

**Jinho Song, Ikkyu Park, Yongseung Sin, Jonghwan Kim, Seongwan Hong, Byungtae Min, and Heedong Kim**
Korea Atomic Energy Research Institute
150 Dukjin-dong, Yuseung-gu, Daejon 305-353, Korea

(Received December 18, 2001)

**Abstract**

The present paper reports spontaneous steam explosions observed in fuel coolant interaction experiments using prototypic reactor materials. Pure $ZrO_2$ and a mixture of $UO_2$ and $ZrO_2$ are used. A high temperature molten material in the form of a jet is poured into a subcooled water pool located in a pressure vessel. An induction skull melting technique is used for the melting of the reactor material. In both tests using pure $ZrO_2$ and a mixture of $UO_2$ and $ZrO_2$, either a quenching or a spontaneous steam explosion was observed. The morphology of debris and pressure profile clearly indicate the differences between the qunching cases and explosion cases. The dynamic pressure, dynamic impulse, water temperature, melt temperature, and static pressure inside the containment chamber were measured. As the spontaneous steam explosion for the reactor material is firstly observed in the present experiments, the results of present experiments could be a siginificant step torward the understanding the explosivity of the reactor material.

**Key Words** : reactor material, steam explosion, TROI, $UO_2/ZrO_2$

## 1. Introduction

In the course of severe accidents at nuclear power plants, the fuel in the core could melt and relocate to the bottom of the reactor vessel. It would result in an interaction of high temperature molten fuels with water. It involves a rapid transfer of energy from the molten fuel to the surrounding water [1]. It is called Fuel and Coolant Interaction (FCI). It might happen during the flooding a degraded core or when a molten core drops into the lower vessel head filled with water, or when molten core debris is ejected into the wet reactor cavity after the vessel failure or the molten debris is flooded in the containment. Each of these scenarios may lead to an energetic FCI process in a time scale ranging from milliseconds to hours. Interactions occurring in a millisecond range can lead to the energetic steam explosions, which could threaten the integrity of the reactor vessel and containment. Interactions occurring in a longer range are normally non-energetic, and are characterized by partial fragmentation and quenching of melt.

Experimental research on FCI has been performed during the last decades in a wide range

including single drop fragmentation [2], intermediate scale experiments, and experiment using prototypic materials. FITS [3], ZREX [4], and ALPHA [5] belong to intermediate scale experiments. FARO [6,7], KROTOS [8,9] and COTELS [10] belong to experiments using prototypic materials. The major accomplishment of previous research is that the probability of alpha-mode failure is very low and can be considered resolved from the risk perspective. The consequence of FCIs seems to be not catastrophic as previously thought. The remaining issue is the structural loading of the lower head due to water-onto-melt steam explosions in the new plant designs relying on in-vessel retention (IVR) and the the explosivity of the reactor material. Recently, a FCI research under OECD/NEA is initiated to investigate this issue.

Korea Atomic Energy Research Institute (KAERI) started a research program on the steam explosion experiment named "Test for Real cOrium Interaction with water (TROI)" in 1997. The objective of the program is to investigate whether the corium would lead to an energetic steam explosion when interacted with cold water at low pressure and to measure the conversion ratio of the energetic steam explosion, if it occurs. This experimental program is pursued not only to investigate the fundamental issue of the explosivity of reactor material but also to contribute to the development of APR1400. As APR1400 considers external cooling of the reactor vessel as an IVR strategy, an ex-vessel steam explosion is possible when there is a breach of reactor vessel pressure boundary.

## 2. Experimental Facility and Cold Crucible

The test facility consists of an upper vessel, lower vessel of a containment chamber, a sliding valve, and a test section in the lower containment chamber as shown in Fig. 1. The upper vessel contains the crucible and melt release assembly. A high temperature molten material is poured into the test section. The configuration and tagging for the instrumentation are also indicated in Fig. 1.

Piezoelectric pressure transducers (PCB piezotronics inc., model 112A, maximum pressure 69 MPa, rise time 2μs, and resonant frequency 250 kHz) are mounted on the wall of the test section and the pressure vessel to measure the dynamic pressure. The static pressure transducer (Druck Co., model pmp 4060, maximum pressure 3.5 Mpa, response time 1 kHz) measures the transient pressure inside the test vessel and containment chamber. The VXI system (800 kHz sampling/channel, 1 kHz/channel) by Agilent Technology is used for the data acquisition. The transient data are acquired at two different frequencies of 100 Hz and 50 kHz by one control program. The high-speed digital video imaging system (Phantom V 4.0, 512×512 pixels at 1000 pps) captures the pictures of explosive fuel coolant interaction. CCD (Charge-Coupled Device) cameras at 4 locations (two in the lower vessel, two in the upper vessel) monitor the sequence of the events for the experiments.

The melting and melt release techniques are necessary for FCI experiment. As the melting temperature of corium is extremely high, an implementation of the melting technique encounters many engineering problems. To solve this problem, an induction skull melting technique, which was originally developed by P. N. Lebedev Institute of the Academy of Sciences of the USSR [13], is utilized. It provides greater purity and flexibility when working with reactive materials. The major design parameters and process of developing induction skull melting technique for this experiment are discussed in Hong et. al. [14]. The RF (Radio Frequency) generator used in the

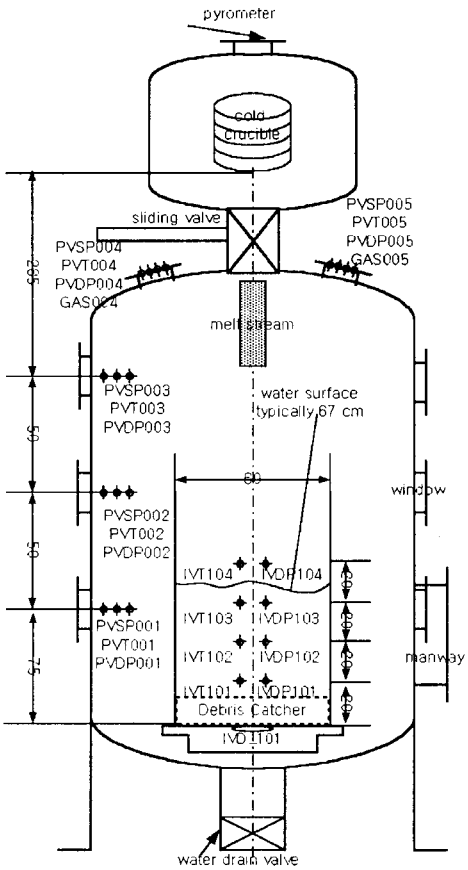


**Fig. 1. A Schematic Diagram of TROI Facility**

TROI test facility has a capacity of 150 kW and frequency of 50 kHz. The frequency of RF generator and the impedance of working coil are selected have a best coupling between the target material and magnetic flux for a $UO_2/ZrO_2$ mixture at 8:2 composition. The cold crucible designed for the $UO_2/ZrO_2$ mixture are used for the melting of both pure $ZrO_2$ and $UO_2/ZrO_2$ mixture.

The cold crucible and melt release assembly, which consists of a plug and a puncher are mounted in the upper vessel of the containment chamber. The palisade-like wall of the cold crucible is made of copper tubes, in which sub-cooled water is supplied for cooling. The plug, whose diameter is 80 mm, is located at the

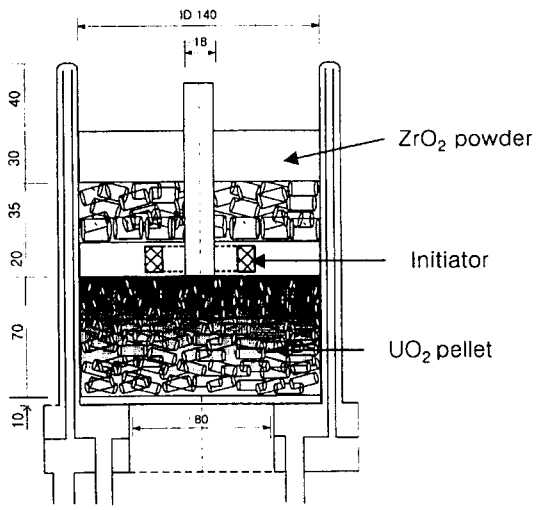


**Fig. 2 Cold Crucible Charged with Mixture**

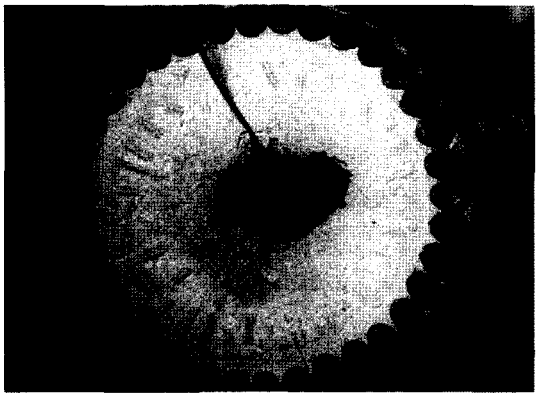

**Fig. 3(a). Top View of the Cold Crucible**

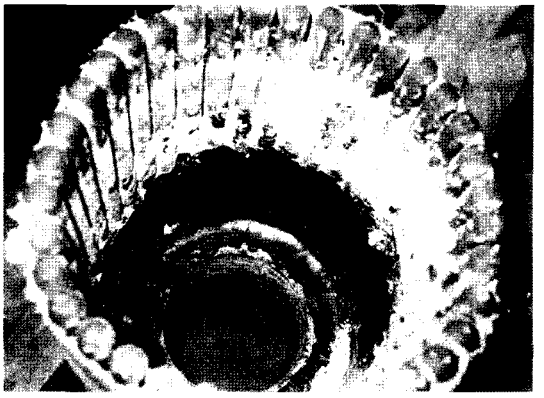

**Fig. 3(b). Inside the Cold Crucible**

bottom of the crucible. After the plug is removed for melt delivery, the conical-shaped puncher punches the crust formed at the bottom of melt to initiate the melt discharge.

A schematic diagram of the cold crucible charged with $UO_2/ZrO_2$ mixture is shown in Fig. 2.

As shown in the figure, $UO_2$ pellet and $ZrO_2$ powder are used for charging. Various charging patterns are tested for efficient melting. The charging pattern in Fig. 2 is one of the best configurations for the efficient coupling between the mixture and magnetic flux. The mass of initial charging is about 14 kg with 70 weight percent of $UO_2$ pellet and 30 weight percent of $ZrO_2$ powder. Zr ring, whose weight is 0.1 kg, is placed in the middle of the crucible. It is used as an initiator. The copper tube initially inserted at the center of the crucible is taken out after the completion of charging to make an artificial hole. The hole is maintained during the melting period, which is used as a view port for the pyrometer.

Fig. 3(a) and (b) show the typical shape of the crucible after the melt is delivered to the water pool. As shown in Fig. 3(a), a crust made of $ZrO_2$ powder is formed on the top of the crucible. A hole is maintained on the top of the crust during the melting period. In Fig. 3(b), inside of the crucible is shown after the top crust is removed. It is shown that a thin crust formed near the bottom portion of the crucible, the thickness of which is about 2-3 mm. It insulates the high temperature molten corium pool from the copper tube at room temperature. A hole punched for the melt delivery is shown at the bottom of the crucible.

An optical two-color pyrometer (Chino co., IR-AQ, resolution : 2℃, 1100~3100℃) measures the melt temperature in the furnace. The pyrometer views the melt pool through a hole formed in the upper crust of the melt. During the melting process, the melt temperature was measured using the two-color pyrometer. A number of K-type thermocouples are used to measure temperatures in the test section, in the pressure vessel atmospheric space, and in the inlet and exit cooling line of the induction coil.

## 3. Results of FCI Experiments Using Zirconia

Experiments on the interaction between molten $ZrO_2$ and water at various temperatures are performed in the first series of tests in TROI. $ZrO_2$ is a reactor material and similar to $UO_2$ in terms of thermo-physical properties and a much better simulant of $UO_2$ than Alumina as shown in Table 1.

**Table 1. Thermo-physical Properties of Molten Material**

| | Corium | $ZrO_2$ | Alumina |
|---|---|---|---|
| Density (kg/m$^3$) | 7,990 | 5,990 | 2,600 |
| Specific Heat (kJ/kg · K) | 0.533 | 0.815 | 1.4 |
| Conductivity (W/ m · K ) | 3.45 | 1.4 | 8 |
| Melting temperature(K) | 2,873 | 2,973 | 2,325 |
| Heat of Fusion (MJ/liter) | 3.17 | 4.23 | 4.05 |

### 3.1. Occurrence of Spontaneous Steam Explosion

Among 6 tests, energetic spontaneous steam explosion has occurred in three tests [15, 16]. As discussed in reference 16, it is the first experiment in the world showing a spontaneous steam explosion for the reactor material. Here, a comparison between a typical quenching test of TROI-3 and the case with energetic steam explosion of TROI-5 is discussed.

The free volume of the containment chamber below the isolation valve is 8.173 m$^3$. The containment chamber is initially at atmospheric pressure. The cross section of the test vessel is rectangular. The dimension is 65cm × 65cm. The height is 150 cm. The initial water level is maintained at 67cm, which is about 283 kg. The free fall height of the melt from the exit of the crucible to the water surface in the test section is about 3.8 m. As the distance between the bottom of the reactor vessel and the cavity floor is about 7 m in APR-1400, the free fall height in this experiment is relevant to the reactor condition.

**Table 2. Initial Conditions and Results for TROI-$ZrO_2$ Tests**

| | TROI test number<br>Date | Unit<br>12/17/00 | 3<br>01/30/01 | 5 |
|---|---|---|---|---|
| Melt | Temperature | [K] | >3373 | >3373 |
| | Charged mass | [kg] | 7.8 | 6.4 |
| | Released mass | [kg] | 4.88 | 2.9 |
| | Initial jet diameter | [m] | 0.060 | 0.04 |
| Test | Water mass | [kg] | 283 | 283 |
| | Sub-cooling | [K] | 50 | 36 |
| Results | Maximum pressurization | [MPa] | 0.01 | 0.035 |
| | Time to reach peak | [sec] | 6 | 1 |
| | Maximum PV heat-up | [K] | 25 | 40 |
| | Time to reach peak | [sec] | 30 | 1 |
| | Steam explosion | | SS | SE |
| | Dynamic pressure peak | [MPa] | 0.07 | 1.0 |
| | Duration | μsec | 50 | 50 |
| Debris | Total amount | [kg] | 4.88 | 3.02 |
| | Crust(>50mm) | [kg] | 2.56 | 0.62 |
| | Crust(10~20mm) | [kg] | - | 0.58 |
| | Particle(10~20mm) | [kg] | 1.12 | 0.04 |
| | Particle-dominated(2~5mm) | [kg] | 0.77 | 0.74 |
| | Particle(710m~2mm) | [kg] | 0.35 | 0.54 |
| | Fine particle(<710 mm) | [kg] | 0.08 | 0.5 |

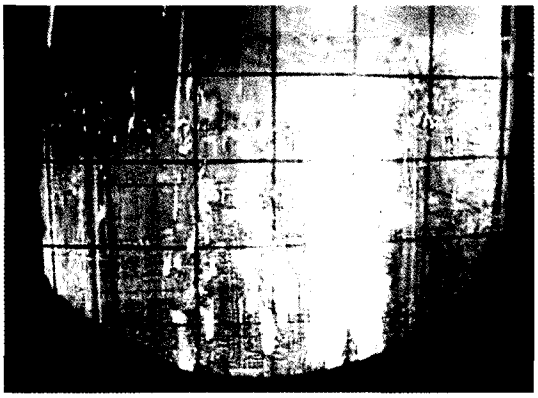

**Fig. 4. Video Image of the $ZrO_2$/water Mixture Just Before the Steam Explosion**

Other initial conditions and the results of experiments are shown in Table 2. As we used a test section made of poly-carobonate walls with stainless steel frame, we were able to take the picture of the interaction process by high-speed video and home video cameras. However, as the melt was very bright, it was necessary to adjust the exposure and to use a neutral density filter or a polarized filter. The windows of the test section are broken and the steel frames are largely defomed in TROI-5 test, while the test section in TROI-3 remained intact.

Fig. 4 shows the home video image of melt-water interaction just before explosion in TROI-5 test. Just in the next frame of the home video image, an energetic steam explosion occurred and the test section is totally broken. The cell size is 10 cm x 10 cm. It is suggested that the effective size of the melt jet and water interaction zone is about 20 cm before the explosion.

### 3.2. Dynamic Pressure

The dynamic pressures were measured for the TROI-3 and TROI-5 experiments. In TROI-3 test, the test section remained intact and the measure peak pressure was very small, less than 0.1 MPa. We called it steam spike (SS). In TROI-5 test, a loud sound was heard outside the pressure vessel and the test section containing the water was broken. Another test of TROI-6 was performed by using a cylindrical stainless steel container to avoid damage to the test section. It has 40cm diameter and 80cm height. The thickness of the wall was 5

**Table 3. Initial Condition and Results for TROI-$ZrO_2$ Tests**

| | TROI test number | Unit, Date | 6, 03/21/01 |
|---|---|---|---|
| Melt | Temperature | [K] | >3373 |
| | Charged mass | [kg] | 8.2 |
| | Released mass | [kg] | 4.23 |
| | Initial jet diameter | [m] | 0.04 |
| Test | Water mass | [kg] | 84 |
| | Sub-cooling | [K] | 81 |
| Results | Maximum pressurization | [MPa] | 0.022 |
| | Time to reach peak | [sec] | 1 |
| | Maximum PV heat-up | [K] | 25 |
| | Time to reach peak | [sec] | 2 |
| | Steam explosion | | SE |
| | Dynamic pressure peak | [MPa] | 12 |
| | Duration | μsec | >100 |

**Fig. 5 Broken Test Section for TROI-6**

mm and the thickness of the bottom plate was 10 mm. The initial conditions and results of the TROI-6 tests are shown in Table 3.

Other conditions are the same as those of TROI-5. Unexpectedly, the stainless steel container was totally broken along the welding line as shown in Fig. 5. Fig. 6 (a) and (b) show the measured dynamic pressure wave profiles for TROI-5 and TROI-6 tests. IVDP stands for the dynamic load cell located on the wall of the test section as shown in Fig. 1 and PVDP stands for the dynamic load cell located on the wall of the pressure vessel.

The time in the fihures are measured from the time of dynamic data acquisition for convenience. It is noted that the smaller container with rigid constraint resulted in a much higher dynamic pressure, which is in the same trend as that of the previous experiments using simulants (Park, Chapman, and Corradini 1999). The results of TROI-6 clearly indicated the occurrence of energetic spontaneous steam explosion for Zirconia and water interaction.

### 3.3. Debris Distribution

After the test, the debris was collected and analyzed using meshes at sizes 20mm, 5mm, 2mm, and 710 μm. The results are summarized in Table 2. There is a clear difference between the case with steam explosion (TROI-5) and the case with steam spike or quenching (TROI-3). The 10-20 mm pebbles do not appear in the explosive case, which is believed to be present in the pre-mixture stage. When it is triggered, the pebbles are finely fragmented and they lead to energetic steam explosion. When it is damped, the pebbles are quenched and maintain their shape. The fine particles at sizes below 0.71 mm seem to be generated during the steam explosion. So, the magnitude of the mechanical energy of steam explosion might be proportional to the amount of fine particles. Unfortunatley, the debris was not collected for TROI-6.

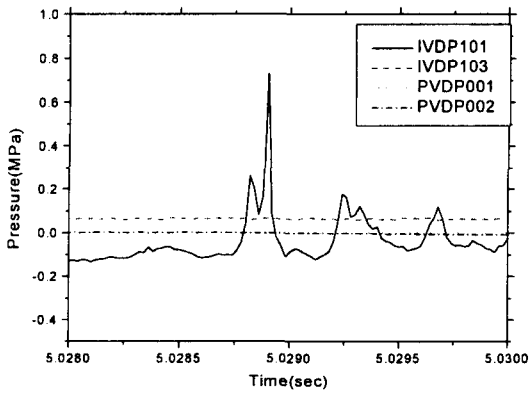


**Fig. 6(a). Dynamic Pressure for TROI-5**

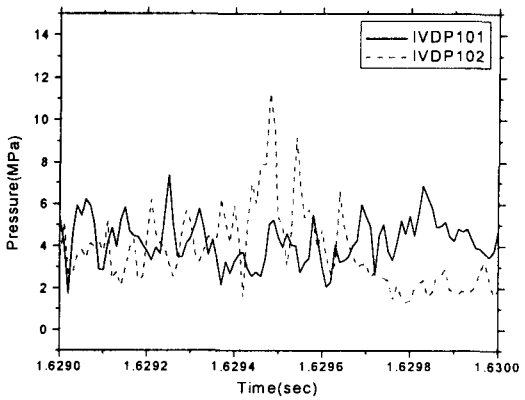


**Fig. 6(b). Dynamic Pressure for TROI-6**

### 3.4. Melt Temperature

The melt temperature was measured by using a two-color pyrometer. The melt temperature turned out to be higher than the upper range of the pyrometer, which is 3373 °K. As the melting temperature of Zirconia is about 3000 °K, the melt seems to have more than 400 °K superheat. There is a strong convection in the melt due to an interaction of the magnetic flux and induced current in the melt [17]. So, it is suggested that there might not be much superheat. Also, as the measured temperature is based on the assumption that the melt is gray body, there could be

**Table 4. Initial Conditions and Results of Corium Tests**

| | TROI test number | Unit, Date | 11, 9/20/01 | 13, 10/22/01 |
|---|---|---|---|---|
| Melt | Initial Charge Composition $UO_2$ / $ZrO_2$ /Zr | [w/o] | 69/30/1 | 69/30/1 |
| | Temperature | [K] | >3373 | > 3300 |
| | Charged mass | [kg] | 13.7 | 13.7 |
| | Initiator mass | [kg] | 0.1 | 0.1 |
| | Released mass | [kg] | 9.185 | 7.735 |
| | Initial jet diameter | [m] | - | - |
| Test | Water mass | [kg] | 189 | 189 |
| | Section | Initial Height | [cm] | 67 67 |
| | Final height | [m] | > 60 | 55 |
| | Cross section | [m2] | 0.283 | 0.283 |
| | Initial temperature | [K] | 296 | 292 |
| | Sub-cooling | [K] | 77 | 81 |
| Results | Maximum pressurization | [MPa] | 0.01 | 0.016 |
| | Time to reach peak | [sec] | 3 | <1 |
| | Maximum PV heat-up | [K] | 50 | 23 |
| | Time to stabilize | [sec] | 20 | <1 |
| | Maximum water heat-up | [K] | 20 | 24 |
| | Time to reach peak | [sec] | 12 | <1 |
| | Steam explosion | | NO | SE |
| | Dynamic pressure peak | [MPa] | - | 7.0 |
| | Duration | msec | - | 1 |
| | Impulse | KN | - | 250 |
| | Duration | msec | - | 15 |
| Debris | Total | [kg] | 9.185 | 7.735 |
| | >6.35mm | [kg] | 1.49 | 0.620 |
| | 4.75mm ~ 6.35mm | [kg] | 1.365 | 0.245 |
| | 2.0mm ~ 4.75mm | [kg] | 4.8 | 2.675 |
| | 1.0mm ~ 2.0mm | [kg] | 1.25 | 1.225 |
| | 0.71mm ~ 1.0mm | [kg] | 0.235 | 0.540 |
| | 0.425mm ~ 0.71mm | [kg] | 0.04 | 0.965 |
| | <0.425mm | [kg] | 0.05 | 1.465 |

uncertainties due to deviations from the gray body.

## 4. Results of FCI Experiments Using Corium

Recent steam explosion experiments using prototypic mixtures of $UO_2/ZrO_2$ [6, 7, 8, 9, 10] did not lead to energetic steam explosion. However, as there is no clear explanation for these phenomena yet, the energetics of corium and sub-cooled water interaction at a low pressure is a unresolved issue for the reactor safety. So a second series of tests using a mixture of $UO_2/ZrO_2$ are performed in the TROI facility to revisit the issue. The initial condition and results of experiments are shown in Table 4.

A strong rigid vessel is used for the second series of test. It is a cylindrical test section made of stainless steel. The height of the vessel is 150 cm, the inner diameter is 60 cm. The thickness of the wall is 2 cm and the thickness of the bottom is 3 cm. At the bottom of the test vessel, a load cell (IVDL) is installed to measure the dynamic impulse. The rest of the set up for the test is the same as that of ZrO2 test.

### 4.1. Occurrence of Spontaneous Steam Explosion

Among 5 tests, energetic spontaneous steam explosion occurred in three tests. Here, the comparison between a typical quenching test of TROI-11 and the case with energetic steam explosion of TROI-13 is discussed.

As the interaction vessel is made of stainless steel, it was not possible to visualize the melt water interaction. Instead, the melt jet before entry into the test section was observed by a high-speed video taken at the highest window at the containment shell. Fig. 7(a), 7(b), 7(c), and 7(d) show the sequential pictures of melt jet delivery for TROI-13. Fig.7 (a) shows a stream of the melt falling into the interaction vessel. The time shown on the picture is measured from the actuation of the puncher. Fig.7 (b) shows the steam flow coming from the interaction vessel, produced by the interaction between the melt and water. Fig.7(c) shows the initiation of splashing of water due to the steam explosion. Finally, Fig.7 (d) shows a column of two-phase mixture and debris expelled by the steam explosion. As we can see, the steam explosion has occurred during the melt delivery. The calibrated size of the picture is 15cm. So, the melt jet diameter at location is about 2cm. As the melt jet is being accelerated by gravity, the melt jet diameter in the water pool would be less than 2 cm.

A mild expulsion of the water column is also observed in TROI-11 test at about 1300 ms, which is due to the vigorous steam generation. The water level for this test is maintained above 60cm, while that of TROI-13 decreased to 55cm.


**Fig. 7. The Sequential Pictures of Melt Jet Delivery**

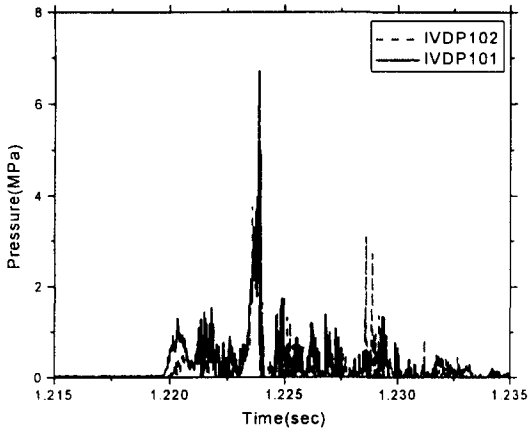


**Fig. 8 Dynamic Pressure of TROI-13**

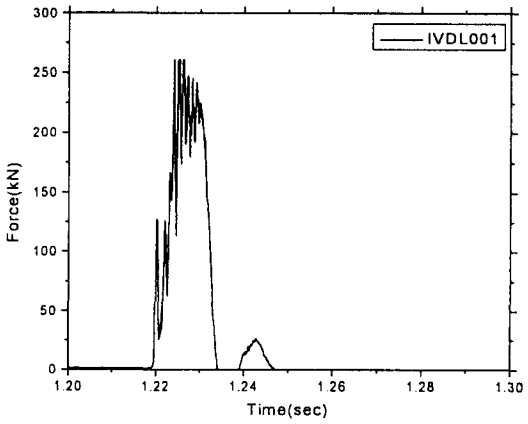


**Fig. 9 Dynamic Impulse of TROI-13**

### 4.2. Dynamic Pressure and Impulse

The dynamic pressure and impulse were measured in TROI-13 test. The puncher was actuated at 6608.82 second after the start of melting. Fig.8 shows the dynamic pressures in the interaction vessel. In the interaction vessel, the peak pressure of 7.0MPa is measured. After the puncher, it took 1.22 second for the occurrence of energetic steam explosion. The peak pressure was much higher than that of TROI-12.

It is noted that there are several peaks indicating multiple explosions. The duration of the highest dynamic pressure is about 1ms. The multiple steam explosions are possible as the melt jet is continuously fed after the initiation of the steam explosion as shown in Fig. 7.

It is worthwhile to look into the location and timing of steam explosion. As the hole is maintained in the upper crust, the molten pool is at atmospheric pressure. It suggests that the melt jet is delivered by gravity alone. Then, the velocity of melt and travel distance can be calculated. The leading edge of the melt jet is first visualized at about 1000ms after the actuation of puncher. As the location of the view port is 2.408 m below the exit of the crucible, the time delay for the initiation of coherent melt jet delivery is calculated as 300ms. The time to hit the water surface is calculated as 1133ms. Fig. 8 below indicates that the initiation of a steam explosion is at about 1220ms. If we assume that the melt is not decelerated after the entry of water pool, the time to hit the bottom is 1213ms. So, it suggests that the steam explosion might have occurred either in the water pool or at the bottom of the tank and that it took 100 ms to form pre-mixture to initiate spontaneous steam explosion.

Fig.9 shows the dynamic load beneath the interaction vessel. The dynamic load was measured up to higher than 250kN, the upper limit of the dynamic load cell and then cut off. The duration of the dynamic load is about 15 ms. As the impulse is an integral behavior of water inside the interaction vessel, the shape of impulse and dynamic load is rather different.

### 4.3. Debris Distribution

The TROI-11 tests did not lead to the spontaneous steam explosion, though the measure melt temperature was above 3373 °K. So, we

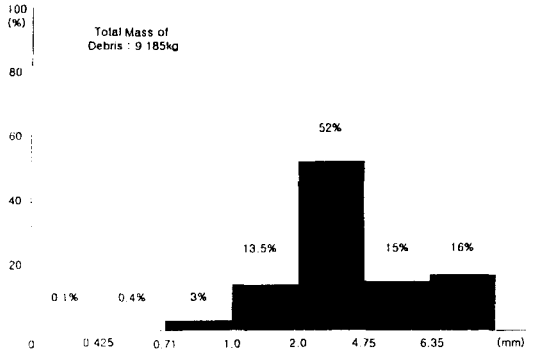


**Fig. 10 Debris Configuration of TROI-11**

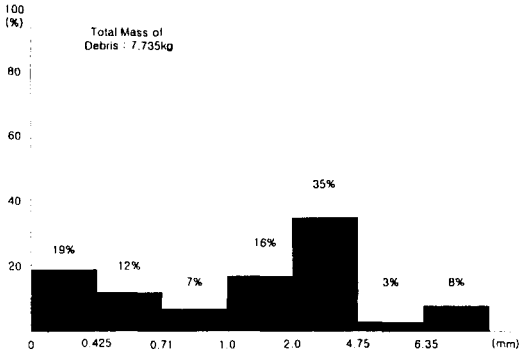


**Fig. 11 Debris Configuration of TROI-13**

looked at the debris configuration to find out the reason for the non-explosive interaction.

After the test, the released melt was collected and examined. A lot of $UO_2$ pellets in their original shape were observed in the collected debris from the water pool. It indicates that although the surface temperature of the melt had been measured high enough to melt the corium mixture, the mixture had not been fully melted due to the short melting time. It might be the reason why a steam explosion did not occur in this test. The size of debris collected after the melt-coolant interaction was measured using sieves. It is shown in Table 4 and Fig.10.

The size of the largest debris containing the unmelted $UO_2$ pellets was about 10mm and the average size of the debris was 2-5mm. They are much smaller than those collected from $ZrO_2$ test whose size ranges from 50mm to 100mm. The fine debris at sizes below 0.71 mm do not exist. It indicates that there was not an energetic interaction. There could have been mild pressure spikes, which have pushed the water out of the test vessel.

The size of debris collected for TROI-13 is shown Table 4 and Fig.11. There also exist $UO_2$ pellets, which were not fully melted. However, the amount was much smaller than that of TROI-11. It indicates that the melt temperature of this test might be higher than that of TROI-13.

The largest debris was about 10mm and the average size of the debris was 1-5mm. They are much smaller than those collected from $ZrO_2$ test whose size ranges from 50mm to 100mm. It is clearly noticed that the fine debris was produced in TROI-13 due to a steam explosion. The amount of melt debris at sizes below 0.71 mm is about 31 %, while the debris at this size did not exist in TROI-11.

### 4.4. Melt Temperature

Similar to the results of the $ZrO_2$ tests, the melt temperature exceeded the upper range of the pyrometer in all five corium tests except TROI-13 test. In TROI-13 test, the measured temperature decreased after it reached 3300 °K, while the gas was discharged from the hole. If the sizes of particles are similar to the measuring wavelengths, which are 0.8μm and 0.96μm, the accuracy of the two-color pyrometer could be heavily influenced by the hot discharge gas. Because the power input to the cold crucible was continously increased even after the measured temperature reached 3300 °K and the debris

disrtibution of TROI-13 indicated much less unmelted $UO_2$ pellets, the actual temperature is belived to be higher than 3300 °K.

### 4.5. Comparison with FARO L-31

The FCI experiments performed under FARO and KROTOS program did not lead to the spontaneous steam explosion, while TROI does. Among those tests, FARO L-31 is most similar to the TROI-13 test. Table 5 shows comparison of those two tests.

There are two major differences. One is melt temperature. And the other is the hydrogen generation. In the FARO tests, the melt superheat was not high, while the melt superheat seems to be high enough is the TROI tests, though there are uncertainties in the pyrometer measurement. Significant amount of hydrogen generation was observed in the FARO tests. However, the hydrogen generation was negligible in the TROI tests.

**Table 5. Comparison of FARO L-31 and TROI-13**

| | L-31 | TROI-13 |
|---|---|---|
| Melt Mass (kg) | 92 | 7.7 |
| Composition ($UO_2/ZrO_2$) | 80:20 | 70:30 |
| Melt Temperature (K) | 2990 | > 3300 |
| Melt Release Diameter (mm) | 50 | 20 |
| Test Section Diameter (m) | 0.71 | 0.6 |
| Initial Pressure (MPa) | 0.21 | 0.1 |
| Atmosphere | Argon | Air |
| Free Board Volume ($m^3$) | 3.54 | 8.03 |
| Melt Fall Height (m) | 0.74 | 3.9 |
| Water Depth (m) | 1.45 | 0.67 |
| Water Temperature (K) | 291 | 292 |
| Debris | < 1mm, ~5% | < 1mm, ~40% |

## 5. Discussions

The fact that spontaneous energetic steam explosions are observed in the FCI experiment using reactor material draws attention, as it is quite different from previous experiments of FARO, KROTOS, and COLTELS. So, here we disscuss the differences between the previous experiments and present experiments and potential reasons affecting the explosivity of corium.

The first one is the amount of hydrogen generation during the fuel coolant interaction. FARO had a considerable amount of hydrogen generation [6], while TROI experiments using corium produced only negligible amount of hydrogen. Though the reason for the difference in hydrogen generation is not clear yet, it might have affected trigger mechanism.

The second one is the amount of superheat. While the superheat of the melt above melting temperature in the KROTOS and ZREX is below 300 °K, the superheat for the present experiment is expected above 400 °K. However, as the results of the WFCI experiment for the simulant [14] indicated that the cut-off temperature for a spontaneous explosion is not very sensitive to the fuel temperature, it might have little efect.

The third one is the pool geometry. The test section of the KROTOS is a kind of one-dimensional shape, where a cylindrical test section with a 200mm inner diameter is used. The initial jet diameter in the KROTOS experiment is about 30 mm, which leads to a water to fuel ratio of 30 in terms of the cross sectional area. As the initial melt jet diameter of this test is about the same as that of KROTOS, TROI provides bigger water to melt cross-sectional area ratio. It is judged to be better for the spontaneous steam explosion in two aspects: It provides enough water volume for the melt water interaction, and it provides enough flow area for the venting of steam generated from

the leading portion of the melt jet. They would reduce the average steam void fraction in the melt water interaction zone.

Though we cannot make a conclusive answer yet, it is quite possible that these three differences might have lead to the spontaneous steam explosion of the reactor material. Further investigations are planned including a sensitivity study on the initial conditions of the experiment, and a detailed measurements by advanced instrumentations.

## Acknowledgments

The authors appreciate the support from the Ministry Of Science and Technology of the Korean Government.

## References

1. M. L. Corradini, B. J., Kim, B. J. and M. D., Oh, "Vapor Explosions in light water reactors: A review of theory and modeling," Progress in Nuclear Energy, Vol. 22, No. 1, pp.1-117, (1988).
2. X. Chen, R. Luo, W. W. Yuen, and T. G. Theofanous, "Experimental simulation of microinteractions in large scale explosions," Proc. of the OECD/CSNI specialist meeting on fuel coolant interactions, JAERI-Tokai, Japan, 364-390, (1997).
3. D. E. Mitchell, M. L. Corradini, and W. W. Tarbell, "Intermediate scale steam explosion phenomena: Experiments and analysis," SAND81-0124, SNL, (1981).
4. D. H. Cho, D. R. Armstrong, and W. H. Gunther, "Experiments on interactions between Zirconium-containing melt and water," NUREG/CR-5372, (1998).
5. N. Yamano, Y. Maruyama, T. Kudo, A. Hidaka, and J. Sugimoto, "Phenomenological Studies on Melt-coolant Interactions in the ALPHA Program," Nuclear Engineering and Design, Vol. 155, pp. 369~389, (1995).
6. D. Magallon, I. Huhtiniemi, and H. Hohmann, H., "Lessens learnt from FARO/TERMOS corium melt quenching experiments," Nuclear Engineering and Design 189, 223-238, (1999).
7. D. Magallon and I. Huhtiniemi, Corium melt quenching tests at low pressure and sub-cooled water in FARO, Nuclear Engineering and Design, 204, 369-376 (2001).
8. I. Huhtiniemi, D. Magallon, and H. Hohmann, "Results of recent KROTOS FCI tests: Alumina vs. Corium Melts," Proc. of the OECD/CSNI specialist meeting on fuel coolant interactions, JAERI-Tokai, Japan, 275-286, (1997).
9. I. Huhtiniemi, and D. Magallon, "Insight into Steam Explosions with Corium Melts in KROTOS", Proc. of NURETH-9, San-Francisco, California, U.S.A., (1999).
10. M. Kato, H. Nagasaka, Y. Vasilyev, A. Kolodesshnikov and V. Zhdanov, "Fuel coolant interaction tests under ex-vessel conditions", Proc. of the OECD workshop on ex-vessel debris coolabilitty, Karlsruhe, 293-300, (1999).
11. D. Magallon et. al, "Proposal for a OECD research programme on fuel-coolant interaction-Steam Explosion Resolution for nuclear applications," (2001).
12. S. J. Oh, "The role of IVR from the severe accident management perspective," Workshop on In-Vessel Retention for the KNGR Severe Accident Management, KEPRI, Daejon, Korea, (1999).
13. V. I. Aleksandrov, V. V. Osiko and V. M. Tatarintsev, "Otchet FIAN," Moskow, (1968).
14. S. W. Hong, B. T. Min, J. H. Song, H. D. Kim, J. K. Choi, "A Study on the Melting and Release of Refractory Materials using Induction Skull Melting," Proc. of the Second

Japan-Korea Symposium on Nuclear Thermal Hydraulics and Safety, Fukuoka, Japan (2000).

15. J. H. Song et al., "The Preliminary Results of Steam Explosion Experiments in TROI," Paper number 74, 9th International Conference on Nuclear Engineering, April 8-12, Nice, France, (2001).
16. J. H. Song, et al., "Experiments on the interactions of molten ZrO2 with water using TROI facility," Nuclear Engineering and Design, Vol. 213, pp. 97-110 (2002).
17. V. I. Aleksandrov, V. V., Osiko, A. M. Prokhorov , and V. M. Tatarntsev, V. M., "Synthesis and crystal growth of refractory materials by RF melting in a cold container," Chapter 6, Current topics in materials Science, Vol. 1, edited by E. Kaldis, North-Holland publishing company, (1978).
18. H. S. Park, R. Chapman and M. Corradini, "Vapor explosions in a one-dimensional large scale geometry with simulant melts," NUREG/CR-6623, (1999).